Atmos. Chem. Phys. Discuss., https://doi.org/10.5194/acp-2019-471
Manuscript under review for journal Atmos. Chem. Phys.
Discussion started: 23 May 2019

Atmospheric Chemistry and Physics
Discussions

The changing role of organic nitrates in the removal and transport of NO_x

Paul S. Romer Present[1], Azimeh Zare[1], and Ronald C. Cohen[1,2]

[1]Department of Chemistry, University of California Berkeley, Berkeley, CA, 94720, USA.
[2]Department of Earth and Planetary Sciences, University of California Berkeley, Berkeley, CA, 94720, USA.

Correspondence: Ronald C. Cohen (rccohen@berkeley.edu)

Abstract. A better understanding of the chemistry of nitrogen oxides (NO_x) is crucial to effectively reducing air pollution and predicting future air quality. The response of NO_x lifetime to perturbations in emissions or in the climate system is set in large part by whether NO_x loss occurs primarily by the direct formation of HNO_3 or through the formation of alkyl and multifunctional nitrates ($RONO_2$). Using 15 years of detailed in situ observations, we show that in the summertime continental boundary layer the relative importance of these two pathways can be well approximated by the relative likelihood that OH will react with NO_2 or instead with a volatile organic compound (VOC). Over the past decades, changes in anthropogenic emissions of both NO_x and VOCs have led to a significant increase in the overall importance of $RONO_2$ chemistry to NO_x loss. We find that this shift is associated with a decreased effectiveness of NO_x emissions reductions on ozone production in polluted areas and increased transport of NO_x from source to receptor regions. This change in chemistry, combined with changes in the spatial pattern of NO_x emissions, is observed to be leading to a flatter distribution of NO_2 across the United States, potentially transforming ozone air pollution from a local issue into a regional one.

1 Introduction

Nitrogen oxides ($NO_x \equiv NO + NO_2$) play a central role in the formation of toxic air pollutants including O_3 and secondary aerosols. More broadly, NO_x chemistry controls the rates and pathways of atmospheric oxidation by determining the concentration of the three most important tropospheric oxidants: OH, O_3, and NO_3. NO_x emissions also directly contribute to nitrogen deposition in sensitive ecosystems (Fowler et al., 2013). Due to its harmful effects to the environment and human health, NO_x has been the target of emissions control strategies since the 1970s, causing anthropogenic NO_x emissions in the United States to have decreased by a factor of 2 or more over the past 30 years (United States Environmental Protection Agency, 2018). Understanding the consequences of these past changes and predicting the results of future emissions reductions on the atmosphere requires a quantitative description of feedbacks between NO_x concentrations and NO_x chemistry.

After emission to the atmosphere, removal of NO_x occurs through two primary pathways: conversion to HNO_3 and conversion to alkyl and multifunctional nitrates ($RONO_2$). Once formed, HNO_3 is nearly chemically inert in the troposphere, with a lifetime to reaction or photolysis of over 50 hours. HNO_3 is therefore removed almost entirely by wet and dry deposition. $RONO_2$ represents a class of diverse molecules, with atmospheric lifetimes ranging from hours to days depending on the properties of the organic backbone (R-group). The loss of $RONO_2$ is divided among reactions that release NO_x from the R-group and recycle it back to the atmosphere, reactions that result in heterogeneous hydrolysis to form HNO_3, and direct deposition. The latter two pathways permanently remove NO_x from the atmosphere (Nguyen et al., 2015; Romer et al., 2016; Fisher et al., 2016). Other NO_x oxidation products, such as peroxy acetyl nitrate (PAN) or HONO can play an important role in the transport and redistribution of NO_x but do not generally lead to permanent NO_x removal.

Historically, direct HNO_3 production was thought to be the only important NO_x loss pathway, with $RONO_2$ chemistry playing at most a minor role. However, several studies have shown that the formation rate of $RONO_2$ in cities or forested regions can be competitive with or greater than the direct production rate of nitric acid (Rosen et al., 2004; Farmer et al., 2011; Browne et al., 2013; Romer et al., 2016; Sobanski et al., 2017).

The relative importance of HNO_3 and $RONO_2$ production is an important factor in setting the lifetime of NO_x (Romer et al., 2016) and affects the response of NO_x loss to temperature (Romer et al., 2018). Due to their different production pathways, the relative importance of HNO_3 and $RONO_2$ production also controls how NO_x loss and ozone production are affected by changes to emissions of NO_x or volatile organic compounds (VOCs). By terminating the radical chain reactions, the formation of $RONO_2$ serves to suppress ozone formation in polluted areas (Perring et al., 2010; Farmer et al., 2011; Edwards et al., 2013; Lee et al., 2014). Several studies have also shown that $RONO_2$ can efficiently partition into aerosols, potentially explaining a large portion of secondary organic aerosol in a wide range of environments (Rollins et al., 2012; Pye et al., 2015; Xu et al., 2015b; Lee et al., 2016).

Multiple previous studies have used chemical transport models to investigate how the relative production of $RONO_2$ and HNO_3 varies in different environments. Browne and Cohen (2012) modeled NO_x loss over the Canadian Boreal Forest using WRF-Chem and Fisher et al. (2016) and Zare et al. (2018) studied NO_x loss in the southeast United States using GEOS-Chem and WRF-Chem respectively. These studies agree that in rural and forested areas with lower NO_x emissions and higher biogenic VOC emissions, $RONO_2$ chemistry is often the largest sink of NO_x.

However, these studies diverge in their conclusions about the overall importance of $RONO_2$ chemistry as a NO_x sink and how it is likely to change in the future. In a WRF-Chem simulation identical to those described in Zare et al. (2018), $RONO_2$ chemistry is found to be 60 % or more of the total NO_x loss across broad swathes of the southeast United States (Fig. 1), while Fisher et al. (2016) found $RONO_2$ production to be concentrated in rather small sections of the southeast. Furthermore, Fisher et al. (2016) suggested that the contribution of $RONO_2$ chemistry to NO_x loss across the region is unlikely to change significantly in the future due to the spatial segregation of NO_x and VOC emissions. On the other hand, Zare et al. (2018) and Browne and Cohen (2012) suggested that the the contribution of $RONO_2$ chemistry to NO_x loss was likely to grow significantly if anthropogenic NO_x emissions decreased across the United States.

Here we use in situ observations from a collection of 13 different field deployments to investigate how the relative production of $RONO_2$ and HNO_3 varies across the United States and how this fraction may change in the future. We show that the relative production of $RONO_2$ and HNO_3 can be well described by the relative OH reactivity of NO_2 and of the combined VOC mixture. As both anthropogenic NO_x and anthropogenic VOC emissions have decreased substantially in the United States over the past 20 years, the relative role of these two pathways has shifted as well. While the shift has generally been towards an

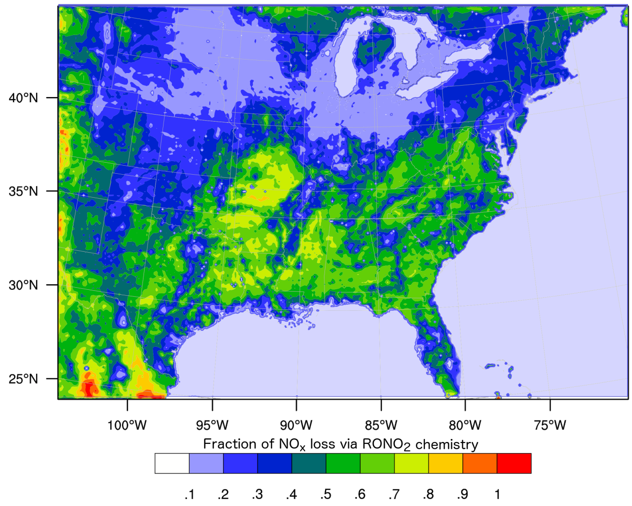

Figure 1. Average (24-hour) fraction of total NO_x loss via $RONO_2$ chemistry over the southeast United States in summer 2013 simulated using the RACM2_Berkeley2 mechanism in WRF-Chem (Zare et al., 2018).

increasing role for $RONO_2$ chemistry, the shift has been smallest in large cities and largest in the transitional regime around them. Combined with changing emission patterns of NO_x, the shift in NO_x chemistry is leading to a flatter distribution of NO_x across the continental United States.

2 NO_x chemistry and production of $RONO_2$ and HNO_3

NO_x is emitted to the atmosphere as NO from a range of anthropogenic and biogenic sources, including motor vehicles, power plants, lightning, fires, and soil bacteria. In the daytime, NO interconverts with NO_2 on a timescale of minutes through Reactions (R1–R2), forming the chemical family NO_x. When NO_x is combined with VOCs and hydrogen oxides (HO_x), a set of linked radical chain reactions is formed (Reactions R3–R6). As part of these reactions, two molecules of NO are oxidized to NO_2, leading to the net production of O_3 through Reaction (R2).

$$\mathrm{NO + O_3 \rightarrow NO_2 + O_2} \tag{R1}$$

$$\mathrm{NO_2} + h\nu + \mathrm{O_2 \rightarrow O_3 + NO} \tag{R2}$$

$$\mathrm{OH + R + O_2 \rightarrow RO_2 + H_2O} \tag{R3}$$

$$\mathrm{RO_2 + NO \xrightarrow{1-\alpha} RO + NO_2} \tag{R4a}$$

$$\mathrm{RO + O_2 \rightarrow R'CHO + HO_2} \tag{R5}$$

$$\mathrm{HO_2 + NO \rightarrow OH + NO_2} \tag{R6}$$

The reactions that propagate the catalytic cycle occur at the same time as reactions that remove NO_x from the atmosphere, terminating the cycle. Direct HNO_3 production occurs through the association of OH with NO_2 (R7). $RONO_2$ compounds are produced as a minor channel of the $RO_2 + NO$ reaction (R4b). Some fraction of the time α, these two radicals will associate to form an organic nitrate, with the balance forming NO_2 and eventually producing O_3 (R4a). The branching ratio $k_{R4b}/(k_{R4a} + k_{R4b})$ is designated α and is determined by the nature of the R group as well as the temperature and pressure. Longer carbon backbones and lower temperatures increase α, while lower pressures and oxygenated functional groups decrease it (Wennberg et al., 2018). Typical values of α in the summertime continental boundary layer range from near 0 for small hydrocarbons and highly oxygenated compounds to over 0.20 for large alkanes and alkenes (Perring et al., 2013).

$$\mathrm{OH + NO_2} + M \rightarrow \mathrm{HNO_3} + M \tag{R7}$$

$$\mathrm{RO_2 + NO} + M \xrightarrow{\alpha} \mathrm{RONO_2} + M \tag{R4b}$$

The total rate of $RONO_2$ production can be calculated from the properties of individual VOCs measured in the atmosphere via Eq. (1). In Eq. (1), $Y_{RO_{2i}}$ represents the yield of RO_2 radicals from VOC oxidation and f_{NO_i} represents the fraction of those RO_2 radicals that react with NO instead of reacting with HO_2 or undergoing unimolecular isomerization (e.g., Teng et al., 2017). f_{NO_i} is close to 1 under polluted or moderately-polluted conditions, but decreases in low-NO_x conditions.

$$P(\mathrm{RONO_2}) = [\mathrm{OH}]\sum_{R_i}[\mathrm{R_i}]\cdot k_{\mathrm{OH+R_i}}\cdot Y_{\mathrm{RO}_{2i}}\cdot f_{\mathrm{NO}_i}\cdot\alpha_i \tag{1}$$

If the contributions from individual VOCs are summed and averaged, the total production of $RONO_2$ can also be calculated from the effective behavior of the VOC mixture via Eq. (2), where VOCR is the sum of all measured VOC concentrations weighted by their reaction rate with OH.

$$P(\mathrm{RONO_2}) = [\mathrm{OH}]\cdot \mathrm{VOCR}\cdot Y_{\mathrm{RO}_{2\mathrm{eff}}}\cdot f_{\mathrm{NO}_{\mathrm{eff}}}\cdot\alpha_{\mathrm{eff}} \tag{2}$$

In a similar fashion, the production of HNO_3 can be calculated via Eq. (3), where NO2R is the NO_2 reactivity, or the concentration of NO_2 multiplied by $k_{\mathrm{OH+NO_2}}$. At 298 K and 1 atm, 10 ppb of NO_2 is equivalent to an NO2R of 2.3 s^{-1}.

$$P(\mathrm{HNO_3}) = [\mathrm{OH}] \cdot [\mathrm{NO_2}] \cdot k_{\mathrm{OH+NO_2}} = [\mathrm{OH}] \cdot \mathrm{NO2R} \tag{3}$$

Total NO_x loss is the sum of the conversion to HNO_3 and conversion to $RONO_2$. The fraction of NO_x loss via $RONO_2$ production can be expressed analytically as Eq. 4.

$$\frac{P(\mathrm{RONO_2})}{P(\mathrm{RONO_2}) + P(\mathrm{HNO_3})} = \left(1 + \frac{1}{\alpha_{\mathrm{eff}} \cdot f_{\mathrm{NO_{eff}}} \cdot Y_{\mathrm{RO_{2eff}}}} \times \frac{\mathrm{NO2R}}{\mathrm{VOCR}}\right)^{-1} \tag{4}$$

The relative production of $RONO_2$ and HNO_3 is seen to be controlled by two factors, the first describing the chemistry of RO_2 radicals (α_{eff}, $f_{\mathrm{NO_{eff}}}$, $Y_{\mathrm{RO_{2eff}}}$), and the second the ratio of NO2R to VOCR, which describes whether OH is more likely to react with a VOC or with NO_2. Because Eq. 4 concerns fractional loss of NO_x, the concentration of OH, which affects $RONO_2$ and HNO_3 production equally, does not appear in the result.

We show below that in the summertime continental boundary layer, the terms describing RO_2 radical chemistry vary significantly less than the NO2R/VOCR ratio, allowing the relative importance of $RONO_2$ and HNO_3 chemistry to be roughly estimated from only a single ratio.

3 Observed contributions of HNO_3 and $RONO_2$ chemistry to NO_x loss

Relative $RONO_2$ and HNO_3 production rates were calculated for 13 separate campaign deployments in the northern hemisphere over the past 20 years. Campaigns were selected that included measurements of NO_x, HNO_3, O_3, HCHO, a wide range of VOCs, and total organic nitrates ($\Sigma RONO_2$). Although they do not include measurements of $\Sigma RONO_2$, ITCT2k2 and CALNEX-P3 were also included to provide a pair of measurements of VOCs and NO_x in the same geographic location separated in time. A list of all campaigns used in this study is given in Table 1. Where available, measurements of OH and HO_2 were used to directly calculate RO_2 formation and loss; when these radicals were not available, OH, HO_2, and RO_2 radical concentrations were calculated iteratively based on the rate of HO_x radical production by O_3 and HCHO photolysis. Equations used to calculate the production and loss of these radicals are given in Appendix A.

The fraction of total NO_x loss occurring via $RONO_2$ chemistry from all 13 of these campaigns is shown in Fig. 2a for points within the continental summertime boundary layer. Despite spanning a large range of environments, all 13 campaigns are well described by a single function of the form $(1 + b \cdot (\frac{\mathrm{NO2R}}{\mathrm{VOCR}})^m)^{-1}$ (red line in Fig. 2a). This roughly matches the expected form if the VOC mixture were constant between environments, and so all parameters other than NO2R/VOCR remained constant (gray line in Fig. 2a). However, the observations exhibit a sharper transition from HNO_3-dominated to $RONO_2$-dominated NO_x loss, likely due to an increase in α_{eff} as NO2R/VOCR decreases.

The calculated increase in fractional NO_x loss via $RONO_2$ chemistry as NO2R/VOCR decreases is matched by an increase in the observed ratio of $\Sigma RONO_2$ to the sum of $\Sigma RONO_2$ and HNO_3 (Fig. 2b). However, the increase in fractional concentrations as NO2R/VOCR decreases is much less than the increase in fractional production. At low NO2R/VOCR ratios, the

Atmos. Chem. Phys. Discuss., https://doi.org/10.5194/acp-2019-471
Manuscript under review for journal Atmos. Chem. Phys.
Discussion started: 23 May 2019

Table 1. Field campaigns used in this analysis

Campaign name	Data Reference	Format	Year	Base of Operations	Date
ITCT2k2	ITCT Science Team (2002)	Airborne	2002	Monterey, CA	22 Apr – 19 May
INTEX-NA	INTEX-A Science Team (2006)	Airborne	2004	Palmdale, CA	2 Jul
				Mascoutah, IL	7 Jul – 14 Jul
				Portsmouth, NH	16 Jul – 10 Aug
				Mascoutah, IL	12 Aug
INTEX-B	INTEX-B Science Team (2011)	Airborne	2006	Houston, TX	4 Mar – 19 Mar
				Honolulu, HI	23 Apr – 28 Apr
				Anchorage, AK	1 May – 12 May
BEARPEX 2007	BEAPREX 07 Science Team (2007)	Ground	2007	Georgetown, CA	15 Aug –10 Oct
ARCTAS-B	ARCTAS-B Science Team (2011)	Airborne	2008	Palmdale, CA	18 Jun – 24 Jun
				Cold Lake, Alberta, CAN	29 Jun – 8 Jul
				Thule, Greenland	8 Jul – 10 Jul
BEARPEX 2009	BEAPREX 09 Science Team (2009)	Ground	2009	Georgetown, CA	15 Jun – 31 Jul
CALNEX-P3	CALNEX Science Team (2002a)	Airborne	2010	Ontario, CA	1 May – 22 Jun
CALNEX-SJV	CALNEX Science Team (2002b)	Ground	2010	Bakersfield, CA	15 May – 30 Jun
DC3	DC3 Science Team (2013)	Airborne	2012	Salina, KS	13 May – 30 Jun
SOAS	SOAS Science Team (2013)	Ground	2013	Centreville, AL	1 Jun – 15 Jul
SEAC4RS	SEAC4RS Science Team (2014)	Airborne	2013	Houston, TX	8 Aug – 23 Sep
FRAPPÉ	FRAPPÉ Science Team (2014)	Airborne	2014	Broomfield, CO	16 Jul –16 Aug
KORUS-AQ	KORUS-AQ Science Team (2018)	Airborne	2016	Pyeongtaek, ROK	1 May – 14 Jun
				Palmdale, CA	17 Jun – 18 Jun

dominant $RONO_2$ species are typically short lived and can undergo heterogeneous hydrolysis to produce HNO_3 (e.g., Browne et al., 2013). This indirect source of HNO_3 can be the greatest source of HNO_3 in forested environments, and leads to the relatively weak dependence of fractional concentration on NO2R/VOCR.

The conclusion that variation in VOC parameters is small compared to the variation in the NO2R/VOCR ratio does not hold outside of the summertime continental boundary layer. In the remote marine boundary layer or in the upper troposphere, α_{eff} is extremely low, as the dominant VOCs produce alkyl nitrates at yields of 0.01 or less (Mao et al., 2009; Perring et al., 2013). Under these conditions, HNO_3 dominates NO_x loss even when NO2R/VOCR is less than 3×10^{-1}.

The trend calculated from the in situ observations matches that found in model simulations, that in areas with high ratios of NO2R to VOCR, HNO_3 is the dominant NO_x sink, but as concentrations of NO_x decrease and concentrations of VOCs increase, the opposite is true. The combined in situ observations show that the importance of $RONO_2$ chemistry to NO_x loss is a non-linear function of the NO2R/VOCR ratio, leading to a sharp transition between the HNO_3-dominated and $RONO_2$-

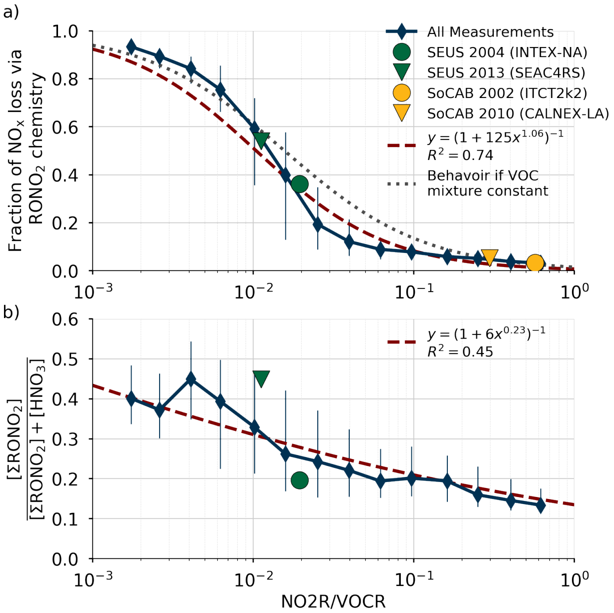

Figure 2. Comparison of the relative production rates of $RONO_2$ and HNO_3 as a function of NO2R/VOCR. Used data points are restricted to the continental summertime boundary layer (i.e., over land, less than 1.5 km above ground level, and average temperature $> 10\ ^{\circ}C$). The top panel shows the fraction of NO_x loss attributable to $RONO_2$ chemistry, as well as a least-squares fit to the data and the expected behavior if α_{eff}, $f_{NO_{eff}}$, $Y_{RO_{2eff}}$ were constant. The bottom panel shows the ratio of $\Sigma RONO_2$ to the sum of HNO_3 and $\Sigma RONO_2$. In each panel, the blue diamonds show the median in each bin and the vertical lines show the interquartile range.

dominated regimes. The sharp transition suggests there is a strong gradient in chemical NO_x loss between urban and rural areas, especially in areas with significant biogenic VOC emissions. Furthermore, the sharp transition indicates that some regions may quickly shift from being HNO_3-dominated to $RONO_2$-dominated if NO2R/VOCR decreases.

Using the trends in Fig. 2a to understand trends in NO_x chemistry over time is only possible if the response to variation across space is equivalent to the response to variation across time. Two direct comparisons of fractional NO_x loss in the same environment but at different times are found to fall along the same curve as the variation between campaigns in different locations (Fig. 2), indicating that such a substitution is valid in this analysis. The first case, INTEX-NA and SEAC4RS, sampled the southeast United States (SEUS) in 2004 and 2013; the second case, ITCT2k2 and CALNEX-P3, sampled the South Coast Air Basin (SoCAB) around Los Angeles in 2002 and 2010. Averages from these pairs of campaigns are shown in Fig. 2a and all four points fall along the same overall curve. For INTEX-NA and SEAC4RS, the shift in chemistry towards the $RONO_2$-dominated regime is accompanied by a dramatic shift in the ratio of $\Sigma RONO_2$ and HNO_3 concentrations, where $\Sigma RONO_2$ concentrations were only one quarter of HNO_3 in 2004 but were nearly equal to HNO_3 in 2013. $\Sigma RONO_2$ measurements are not available for ITCT2k2 or CALNEX-P3, preventing a similar comparison from being made for those campaigns.

Together, these cases indicate that the trend from Fig. 2a can be used to predict changes in fractional loss if the trend in NO2R/VOCR is known. Over the past decade, satellite measurements of NO_2 show a significant decrease in national NO_2 concentrations, reporting an average decrease of 4.5–7 % per year between 2005 and 2011 (Russell et al., 2012). No comparable satellite observations of VOCs exist, but studies in multiple locations have reported a decrease in primary anthropogenic VOC concentrations of 5.5–7.5 % per year over 2000-2010 (Geddes et al., 2009; Warneke et al., 2012; Pollack et al., 2013; Pusede et al., 2014). In contrast, biogenic VOC concentrations have been either constant or increasing over that same time period (Geddes et al., 2009; Hidy et al., 2014). Oxygenated VOCs show no major trend with time, although there are few long-term measurements of these species (Geddes et al., 2009; Pusede et al., 2014).

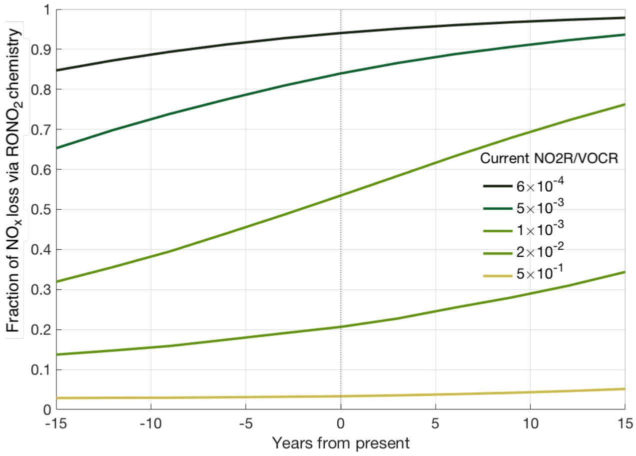

Figure 3. Predicted trends in fractional NO_x loss over time, calculated from the estimated NO2R/VOCR ratio assuming a constant -6.5% yr^{-1} decrease in anthropogenic VOC concentrations, a 5.5% yr^{-1} decrease in NO_x concentrations, and a 1.5% yr^{-1} increase in biogenic VOC concentrations.

These varied trends in NO_x, anthropogenic VOCs, and biogenic VOCs mean that NO2R/VOCR has not changed uniformly over the past decade. Past NO2R/VOCR ratios were calculated by assuming a 6.5% yr^{-1} decrease to anthropogenic VOC concentrations, a 5.5% yr^{-1} decrease to NO_x concentrations, and a 1.5% yr^{-1} increase in biogenic VOC concentrations over the past 15 years. We also extrapolate these same trends to estimate NO2R/VOCR 15 years into the future. The calculated NO2R/VOCR ratios are combined with the relationship from Fig. 2 to estimate fractional NO_x loss at different times (Fig. 3). Based on these trends, $RONO_2$ chemistry is seen to have become a larger portion of total NO_x loss over the past 15 years, although the change is not evenly distributed. The similar trends in NO_x and anthropogenic VOCs cause there to have been little to no change in the regions with the highest NO2R/VOCR ratios (typically large cities). The largest changes are projected to occur in regions with moderate NO2R/VOCR ratios. In these regions, biogenic VOCs often account for a greater fraction of the VOCR, leading to significant decreases in NO2R/VOCR over the past 15 years. In addition, the response of fractional loss to changes in the NO2R/VOCR ratio is magnified in areas where both $RONO_2$ and HNO_3 chemistry contribute to NO_x loss. In this transitional regime, if recent trends continue, the fraction of NO_x loss occurring via $RONO_2$ chemistry could double in the next 15 years. Many regions of the United States are therefore likely to transition from a regime where HNO_3 dominates NO_x loss to a mixed or $RONO_2$-dominated regime.

4 Impacts of the transition from the $\mathbf{HNO_3}$ to the $\mathbf{RONO_2}$ regime

The growing importance of $RONO_2$ chemistry to NO_x loss has several implications for air quality. Most directly, it means that understanding NO_x chemistry in all but the most polluted megacities requires including the effects of $RONO_2$ chemistry. More theoretically, the transition from HNO_3- to $RONO_2$-dominated NO_x loss affects how atmospheric chemistry will respond to changes in emissions of NO_x and VOCs. Because $RONO_2$ are produced in the same set of reactions that produce O_3, the fractional loss of NO_x via $RONO_2$ chemistry is directly proportional to the ozone production efficiency (OPE), the ratio of ozone production to NO_x loss (Eq. 5).

$$\mathrm{OPE} = \frac{P(\mathrm{O3})}{L(\mathrm{NO_x})} = \frac{2\cdot \mathrm{VOCR}\cdot Y_{\mathrm{RO_{2eff}}}\cdot f_{\mathrm{NO_{eff}}}\cdot(1-\alpha_{\mathrm{eff}})}{\mathrm{NO2R}+\mathrm{VOCR}\cdot Y_{\mathrm{RO_{2eff}}}\cdot f_{\mathrm{NO_{eff}}}\cdot\alpha_{\mathrm{eff}}} \propto \frac{P(\mathrm{RONO_2})}{P(\mathrm{RONO_2})+P(\mathrm{HNO_3})} \qquad (5)$$

Fundamentally, OPE represents the total amount of ozone produced for each molecule of NO_x emitted. When considering ozone pollution on regional scales, OPE is a more comprehensive metric than instantaneous ozone production because it accounts for ozone production both locally and further afield.

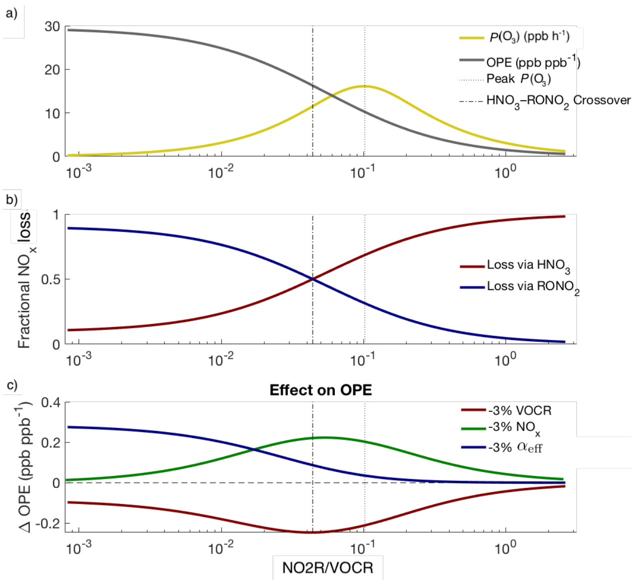

Figure 4. Theoretical picture of NO_x and O_3 chemistry, calculated using variable NO_x concentrations and fixed VOCR, $P(HO_x)$, and α_{eff}. Panel a shows how $P(O_3)$ and OPE change as NO_x changes; Panel b shows how the fractional NO_x loss changes as NO2R/VOCR decreases; Panel c shows that changes to NO_x and VOCR have their greatest effect on OPE not when PO_3 is at a maximum, but at the crossover point between the $RONO_2$-dominated and HNO_3-dominated regimes.

Figure 4 uses the theoretic framework described in Romer et al. (2018) to investigate how ozone and NO_x chemistry change as a function of NO2R/VOCR. As the NO2R/VOCR ratio decreases, OPE increases, reaching an inflection point exactly at the crossover point between the HNO_3-dominated and $RONO_2$-dominated regimes (Fig. 4a–b). For the polluted areas in the country, where HNO_3 is currently the dominant NO_x loss pathway, this means that, for example, interventions to improve air quality by reducing NO_x emissions will be fighting uphill, because every incremental fractional decrease in NO_x emissions will be associated with a growing incremental increase in OPE (Fig. 4c).

In addition, as $RONO_2$ chemistry becomes a more important part of the NO_x budget, changes to α_{eff} have an increasing effect on OPE (Fig. 4c). Policy interventions that reduce VOCR but preferentially target high-α compounds (e.g., long-chain alkanes) could inadvertently increase ozone production or OPE (Farmer et al., 2011; Perring et al., 2013).

In addition to the large effects on aerosol yield that changes to NO_x and VOC emissions have directly (e.g., Xu et al., 2015a; Pusede et al., 2016), they also affect aerosols by changing the fate of NO_x. While both HNO_3 and $RONO_2$ can form aerosols (Stelson and Seinfeld, 1982; Pye et al., 2015), the properties of the resulting aerosols are likely to differ. Because HNO_3 is a strong acid, a shift towards $RONO_2$ chemistry is likely to increase aerosol pH. An increase in the role of $RONO_2$ chemistry will also cause more of the nitrate aerosol to be organic rather than inorganic, potentially affecting the viscosity and morphology of aerosols.

Further effects of changing NO_x chemistry arise from the distinct fates of $RONO_2$ and HNO_3. Many $RONO_2$ compounds, especially those derived from isoprene, are remarkably reactive in the troposphere, with lifetimes of a few hours or less. A fraction of this $RONO_2$ loss returns NO_x to the atmosphere, allowing $RONO_2$ production to effectively transport NO_x downwind (Romer et al., 2016; Xiong et al., 2016). In contrast, HNO_3 is effectively chemically inert in the troposphere, with a chemical lifetime of 50 hours or more.

As a result of the differing chemical fates and lifetimes, transitioning from a HNO_3-dominated regime to a mixed or $RONO_2$-dominated regime has implications for the distribution of NO_x on regional to continental scales. If a greater fraction of NO_x in polluted or moderately polluted regions is converted into $RONO_2$ compounds rather than into HNO_3, then more of the NO_x may be re-released downwind, where it can participate in radical chemistry and ozone production. Simulations of $RONO_2$ chemistry using WRF-Chem and the RACM2_Berkeley2 mechanism (Zare et al., 2018) were used to investigate the $RONO_2$ lifetime and NO_x recycling efficiency of $RONO_2$ across the southeast United States in summer 2013 (Fig. 5). Across much of the region, $\Sigma RONO_2$ are calculated to have a lifetime of roughly 4 hours, and the release of NO_x from $RONO_2$ oxidation was between 40 and 75% of the instantaneous $RONO_2$ production rate. Combined, these findings demonstrate a significant role for $RONO_2$ chemistry in the transport of NO_x between regions in the southeast United States. The effects of organic nitrate chemistry on the distribution of NO_x is likely to vary greatly across different regions of the United States and should be studied in further detail.

Enhanced NO_x transport between source and receptor regions is one aspect of a combined trend that is transforming the spatial distribution of NO_x. Over the past decade, NO_x emission reductions have been concentrated in the most polluted environments. In these areas, motor vehicles and power plants, targets of emission control strategies, account for almost all of the NO_x emissions. In less polluted regions, other sources of NO_x, including soil microbes (both in agricultural and non-

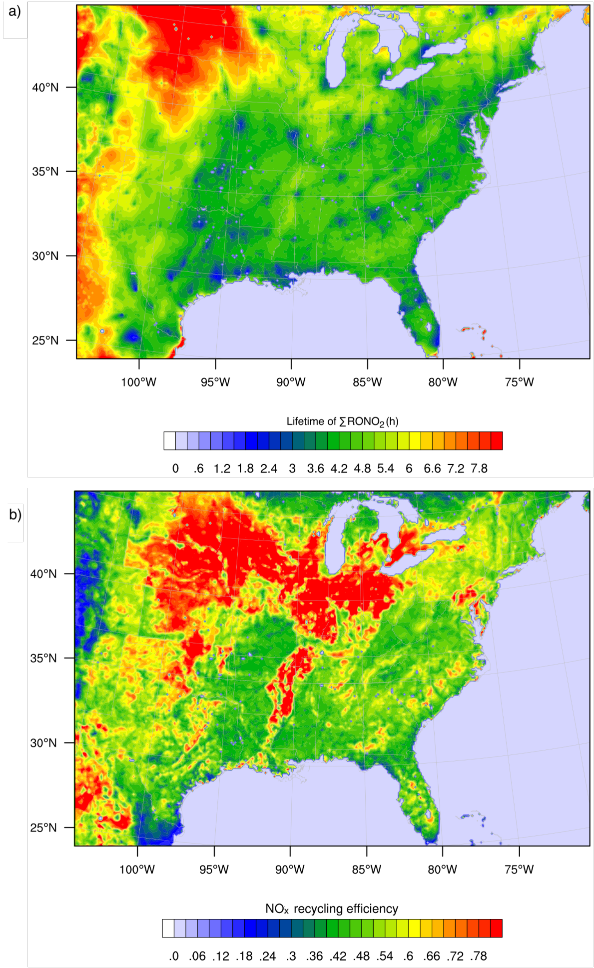

Figure 5. WRF-Chem simulation of $RONO_2$ chemistry over the southeast United States for summer 2013 as described in Zare et al. (2018). Panel a shows the overall lifetime of $\Sigma RONO_2$, defined as the concentration of $\Sigma RONO_2$ divided by their chemical loss rate for the daytime boundary layer. Panel b shows the average NO_x recycling efficiency, defined as the local rate of NO_x production from $RONO_2$ oxidation divided by the rate of $RONO_2$ production.

agricultural regions), off-road vehicles, fires, and lightning, play a greater role in the NO_x budget, reducing the effectiveness of typical combustion-related NO_x emission controls. In addition, hemispheric background concentrations of NO_x and O_3 have risen slightly over the past two decades (Cooper et al., 2012). The combination of all three of these trends suggests that the distribution of NO_x across the United States is getting flatter over time. This trend matches satellite observations of NO_2 over the continental United States. Figure 6 shows the cumulative frequency distribution of summertime tropospheric NO_2 columns from 2005-2007 and 2015-2017 using the BErkeley High-Resolution (BEHR) v3.0A retrieval (Laughner et al., 2018)

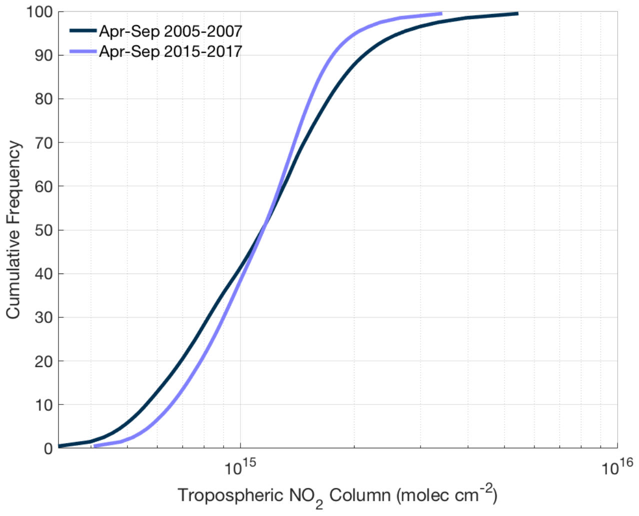

Figure 6. Cumulative frequency distribution of OMI tropospheric NO_2 columns over the continental United States using the BEHR v3.0A retrieval for summer (Apr–Sep) in 2005–2007 and 2015–2017.

of slant-column measurements from OMI. Over this time, the highest percentiles NO_2 concentrations have decreased and the lowest percentiles increased, leading to a significantly narrower distribution of NO_2 concentrations.

In summary, over the past 15 years, decreases in anthropogenic NO_x and VOC emissions have led to a significant shift in the mechanisms of NO_x loss. Many places where HNO_3 production dominated NO_x loss are now mixed or have switched to a situation where the majority of NO_x loss occurs through $RONO_2$ chemistry. If past trends continue, $RONO_2$ chemistry will grow to become an even more important fraction of NO_x chemistry in coming decades. As a result of this combination of changing NO_x chemistry, decreasing NO_x emissions, and increasing background concentrations, air pollution in the United States may transform from a highly local issue to a more extended regional one. Efforts to control air pollution focused only on local sources are less likely to be effective; future improvements in air quality and attaining the most recent National Ambient Air Quality Standards are likely to require coordinated efforts on regional scales to broadly reduce NO_x emissions.

Data availability. Data from ARCTAS, DC3, FRAPPÉ, INTEX-NA, INTEX-B, KORUS-AQ and SEAC4RS are available from https://www-air.larc.nasa.gov/missions.htm. Data from ITCT2k2, CALNEX, SOAS, UBWOS, and WINTER are available from https://www.esrl.noaa.gov/csd/field.html. The BEHR retrieval of OMI NO_2 columns is available at http://behr.cchem.berkeley.edu/.

Appendix A: Calculation of the $RONO_2$ production rate

A1 Steady-state calculation of unmeasured radicals

The formation rates of $RONO_2$, HNO_3, and O_3 depend either directly or indirectly on the concentration of OH, HO_2, RO_2, NO, and NO_2. Speciated RO_2 radicals are not currently observable in the atmosphere, and thus all RO_2 concentrations were calculated assuming they were in steady-state, with their production and loss rates equal.

There were additional periods in which some combination of OH, HO_2, and NO were also not measured, and these radicals were also assumed to be in steady state. Concentrations of VOCs, NO_2, and O_3 were always taken from measurements. In order to calculate the steady-state concentrations of unmeasured radicals, reaction rate constants and RO_2 yields for the different VOCs were taken from the MCM v3.3.1 (Jenkin et al., 2015). Concentrations of all unmeasured species were calculated iteratively until all the concentrations converged. Equations (A1–A7) were used to calculate the steady-state concentration of unmeasured radicals.

$$P(\mathrm{RO_2}) = [\mathrm{OH}]\cdot \mathrm{VOCR}\cdot Y_{\mathrm{RO_2}} \tag{A1}$$

$$L(\mathrm{RO_2}) = k_{\mathrm{RO_2+NO}}[\mathrm{RO_2}][\mathrm{NO}] + k_{\mathrm{RO_2+HO_2}}[\mathrm{RO_2}][\mathrm{HO_2}] + 2k_{\mathrm{RO_2+RO_2}}[\mathrm{RO_2}][\mathrm{RO_2}] + k_{\mathrm{isom}} \tag{A2}$$

$$P(\mathrm{HO_2}) = k_{\mathrm{RO_2+NO}}[\mathrm{RO_2}][\mathrm{NO}](1-\alpha) + [\mathrm{OH}]\cdot \mathrm{VOCR}\cdot Y_{\mathrm{HO_2}} + 2j_{\mathrm{HCHO}} \tag{A3}$$

$$L(\mathrm{HO_2}) = k_{\mathrm{HO_2+NO}}[\mathrm{HO_2}][\mathrm{NO}] + 2k_{\mathrm{HO_2+HO_2}}[\mathrm{HO_2}][\mathrm{HO_2}] + k_{\mathrm{HO_2+RO_2}}[\mathrm{HO_2}][\mathrm{RO_2}] \tag{A4}$$

$$P(\mathrm{NO}) = j_{\mathrm{NO_2}}[\mathrm{NO_2}] \tag{A5}$$

$$L(\mathrm{NO}) = k_{\mathrm{O_3+NO}}[\mathrm{O_3}][\mathrm{NO}] + k_{\mathrm{RO_2+NO}}[\mathrm{RO_2}][\mathrm{NO}] + k_{\mathrm{HO_2+NO}}[\mathrm{HO_2}][\mathrm{NO}] \tag{A6}$$

$$P(\mathrm{OH}) = \frac{2j_{\mathrm{O_3\rightarrow O^1D}}[\mathrm{O_3}]k_{\mathrm{O^1D+H_2O}}}{k_{\mathrm{O^1D+H_2O}}[\mathrm{H_2O}] + k_{\mathrm{O^1D+O_2}}[\mathrm{O_2}] + k_{\mathrm{O^1D+N_2}}[\mathrm{N_2}]} + k_{\mathrm{HO_2+NO}}[\mathrm{HO_2}][\mathrm{NO}] \tag{A7}$$

$$L(\mathrm{OH}) = \mathrm{VOCR} + \mathrm{NO2R} \tag{A8}$$

A2 Determination of α

Accurately calculating the $RONO_2$ production rate requires accurate knowledge of α_i for all VOCs. If values of α had been reported for a specific compound from laboratory measurements, the most recent value was applied (Perring et al., 2013; Teng et al., 2015; Rindelaub et al., 2015; Praske et al., 2015; Wennberg et al., 2018). In cases where no reliable laboratory measurements are available, the parameterization for α from Wennberg et al. (2018) was used. In all cases, the temperature- and pressure-dependencies described in Wennberg et al. (2018) were used to scale the laboratory measurements of α to the conditions of the atmosphere.

Author contributions. PSRP and RCC designed the experiment, PSRP performed the analysis of field campaign data and wrote the paper with contributions from all authors, AZ designed, ran, and analyzed the modeling simulations.

Competing interests. The authors declare that they have no conflict of interest.

Acknowledgements. This study was supported by NOAA grant NA18OAR4310117 in the Atmospheric Chemistry, Carbon Cycle, and Climate program of the NOAA Climate Program Office and by NSF grant AGS-1352972. The authors thank Josh Laughner for assistance with the OMI BEHR retrieval.

References

ARCTAS-B Science Team: ARCTAS-B DC-8 aircraft data, NASA, https://www-air.larc.nasa.gov/cgi-bin/ArcView/arctas, 2011.

BEAPREX 07 Science Team: BEARPEX 2007 field campaign data, 2007.

BEAPREX 09 Science Team: BEARPEX 2009 field campaign data, 2009.

Browne, E. C. and Cohen, R. C.: Effects of biogenic nitrate chemistry on the NO_x lifetime in remote continental regions, Atmos. Chem. Phys., 12, 11 917–11 932, https://doi.org/10.5194/acp-12-11917-2012, 2012.

Browne, E. C., Min, K.-E., Wooldridge, P. J., Apel, E., Blake, D. R., Brune, W. H., Cantrell, C. A., Cubison, M. J., Diskin, G. S., Jimenez, J. L., Weinheimer, A. J., Wennberg, P. O., Wisthaler, A., and Cohen, R. C.: Observations of total $RONO_2$ over the boreal forest: NO_x sinks and HNO_3 sources, Atmos. Chem. Phys., 13, 4543–4562, https://doi.org/10.5194/acp-13-4543-2013, http://www.atmos-chem-phys.net/13/4543/2013/acp-13-4543-2013.html, 2013.

CALNEX Science Team: CALNEX 2010 WP-3D data, NOAA, https://esrl.noaa.gov/csd/groups/csd7/measurements/2010calnex/P3/DataDownload/, 2002a.

CALNEX Science Team: CALNEX 2010 Bakersfield site data, NOAA, https://esrl.noaa.gov/csd/groups/csd7/measurements/2010calnex/Bakersfield/DataDownload/, 2002b.

Cooper, O. R., Gao, R.-S., Tarasick, D., Leblanc, T., and Sweeney, C.: Long-term ozone trends at rural ozone monitoring sites across the United States, 1990–2010, J. Geophys. Res. Atmos., 117, D22 307, https://doi.org/10.1029/2012JD018261, 2012.

DC3 Science Team: DC3 Field Campaign Data from DC-8 aircraft, NASA, https://doi.org/10.5067/aircraft/dc3/dc8/aerosol-tracegas, 2013.

Edwards, P. M., Young, C. J., Aikin, K., de Gouw, J., Dubé, W. P., Geiger, F., Gilman, J., Helmig, D., Holloway, J. S., Kercher, J., Lerner, B., Martin, R., McLaren, R., Parrish, D. D., Peischl, J., Roberts, J. M., Ryerson, T. B., Thornton, J., Warneke, C., Williams, E. J., and Brown, S. S.: Ozone photochemistry in an oil and natural gas extraction region during winter: simulations of a snow-free season in the Uintah Basin, Utah, Atmos. Chem. Phys., 13, 8955–8971, https://doi.org/10.5194/acp-13-8955-2013, 2013.

Farmer, D. K., Perring, A. E., Wooldridge, P. J., Blake, D. R., Baker, A., Meinardi, S., Huey, L. G., Tanner, D., Vargas, O., and Cohen, R. C.: Impact of organic nitrates on urban ozone production, Atmos. Chem. Phys., 11, 4085–4094, https://doi.org/10.5194/acp-11-4085-2011, 2011.

Fisher, J. A., Jacob, D. J., Travis, K. R., Kim, P. S., Marais, E. A., Chan Miller, C., Yu, K., Zhu, L., Yantosca, R. M., Sulprizio, M. P., Mao, J., Wennberg, P. O., Crounse, J. D., Teng, A. P., Nguyen, T. B., St. Clair, J. M., Cohen, R. C., Romer, P., Nault, B. A., Wooldridge, P. J., Jimenez, J. L., Campuzano-Jost, P., Day, D. A., Hu, W., Shepson, P. B., Xiong, F., Blake, D. R., Goldstein, A. H., Misztal, P. K., Hanisco, T. F., Wolfe, G. M., Ryerson, T. B., Wisthaler, A., and Mikoviny, T.: Organic nitrate chemistry and its implications for nitrogen budgets in an isoprene- and monoterpene-rich atmosphere: constraints from aircraft ($SEAC^4RS$) and ground-based (SOAS) observations in the Southeast US, Atmos. Chem. Phys., 16, 5969–5991, https://doi.org/10.5194/acp-16-5969-2016, http://www.atmos-chem-phys.net/16/5969/2016/, 2016.

Fowler, D., Coyle, M., Skiba, U., Sutton, M. A., Cape, J. N., Reis, S., Sheppard, L. J., Jenkins, A., Grizzetti, B., Galloway, J. N., Vitousek, P., Leach, A., Bouwman, A. F., Butterbach-Bahl, K., Dentener, F., Stevenson, D., Amann, M., and Voss, M.: The global nitrogen cycle in the twenty-first century, Philos. T. Roy. Soc. B, 368, https://doi.org/10.1098/rstb.2013.0164, 2013.

FRAPPÉ Science Team: FRAPPÉ C-130 aircraft data, NASA, https://www-air.larc.nasa.gov/cgi-bin/ArcView/discover-aq.co-2014?C130=1, 2014.

Geddes, J. A., Murphy, J. G., and Wang, D. K.: Long term changes in nitrogen oxides and volatile organic compounds in Toronto and the challenges facing local ozone control, Atmos. Environ., 43, 3407–3415, https://doi.org/10.1016/j.atmosenv.2009.03.053, http://www.sciencedirect.com/science/article/pii/S1352231009002507, 2009.

Hidy, G. M., Blanchard, C. L., Baumann, K., Edgerton, E., Tanenbaum, S., Shaw, S., Knipping, E., Tombach, I., Jansen, J., and Walters, J.: Chemical climatology of the southeastern United States, 1999–2013, Atmos. Chem. Phys., 14, 11 893–11 914, https://doi.org/10.5194/acp-14-11893-2014, 2014.

INTEX-A Science Team: INTEX-A DC-8 Aircraft data, NASA, https://doi.org/10.5067/asdcdaac/intexa/0008, 2006.

INTEX-B Science Team: INTEX-B DC-8 aircraft data, NASA, https://doi.org/10.5067/asdcdaac/intexb/0008, 2011.

ITCT Science Team: ITCT 2002 WP-3D Data, NOAA, https://esrl.noaa.gov/csd/groups/csd7/measurements/2002ITCT/P3/DataDownload/, 2002.

Jenkin, M. E., Young, J. C., and Rickard, A. R.: The MCM v3.3.1 degradation scheme for isoprene, Atmos. Chem. Phys., 15, 11 433–11 459, https://doi.org/10.5194/acp-15-11433-2015, http://www.atmos-chem-phys.net/15/11433/2015/, 2015.

KORUS-AQ Science Team: KorUS-AQ Airborne Mission, NASA, https://doi.org/10.5067/Suborbital/KORUSAQ/DATA01, 2018.

Laughner, J. L., Zhu, Q., and Cohen, R. C.: The Berkeley High Resolution Tropospheric NO_2 product, Earth Syst. Sci. Data, 10, 2069–2095, https://doi.org/10.5194/essd-10-2069-2018, 2018.

Lee, B. H., Mohr, C., Lopez-Hilfiker, F. D., Lutz, A., Hallquist, M., Lee, L., Romer, P., Cohen, R. C., Iyer, S., Kurtén, T., Hu, W., Day, D. A., Campuzano-Jost, P., Jimenez, J. L., Xu, L., Ng, N. L., Guo, H., Weber, R. J., Wild, R. J., Brown, S. S., Koss, A., de Gouw, J., Olson, K., Goldstein, A. H., Seco, R., Kim, S., McAvey, K., Shepson, P. B., Starn, T., Baumann, K., Edgerton, E. S., Liu, J., Shilling, J. E., Miller, D. O., Brune, W., Schobesberger, S., D'Ambro, E. L., and Thornton, J. A.: Highly functionalized organic nitrates in the southeast United States: Contribution to secondary organic aerosol and reactive nitrogen budgets, Proc. Natl. Acad. Sci. USA, 113, 1516–1521, https://doi.org/10.1073/pnas.1508108113, 2016.

Lee, L., Wooldridge, P. J., Gilman, J. B., Warneke, C., de Gouw, J., and Cohen, R. C.: Low temperatures enhance organic nitrate formation: evidence from observations in the 2012 Uintah Basin Winter Ozone Study, Atmos. Chem. Phys., 14, 12 441–12 454, https://doi.org/10.5194/acp-14-12441-2014, 2014.

Mao, J., Ren, X., Brune, W. H., Olson, J. R., Crawford, J. H., Fried, A., Huey, L. G., Cohen, R. C., Heikes, B., Singh, H. B., Blake, D. R., Sachse, G. W., Diskin, G. S., Hall, S. R., and Shetter, R. E.: Airborne measurement of OH reactivity during INTEX-B, Atmos. Chem. Phys., 9, 163–173, https://doi.org/10.5194/acp-9-163-2009, 2009.

Nguyen, T. B., Crounse, J. D., Teng, A. P., St. Clair, J. M., Paulot, F., Wolfe, G. M., and Wennberg, P. O.: Rapid deposition of oxidized biogenic compounds to a temperate forest, Proc. Natl. Acad. Sci. USA, 112, E392–E401, https://doi.org/10.1073/pnas.1418702112, http://www.pnas.org/content/112/5/E392, 2015.

Perring, A. E., Bertram, T. H., Farmer, D. K., Wooldridge, P. J., Dibb, J., Blake, N. J., Blake, D. R., Singh, H. B., Fuelberg, H., Diskin, G., Sachse, G., and Cohen, R. C.: The production and persistence of $\Sigma RONO_2$ in the Mexico City plume, Atmos. Chem. Phys., 10, 7215–7229, https://doi.org/10.5194/acp-10-7215-2010, http://www.atmos-chem-phys.net/10/7215/2010/, 2010.

Perring, A. E., Pusede, S. E., and Cohen, R. C.: An Observational Perspective on the Atmospheric Impacts of Alkyl and Multifunctional Nitrates on Ozone and Secondary Organic Aerosol, Chem. Rev., 113, 5848–5870, https://doi.org/10.1021/cr300520x, 2013.

Pollack, I. B., Ryerson, T. B., Trainer, M., Neuman, J. A., Roberts, J. M., and Parrish, D. D.: Trends in ozone, its precursors, and related secondary oxidation products in Los Angeles, California: A synthesis of measurements from 1960 to 2010, J. Geophys. Res. Atmos., 118, 5893–5911, https://doi.org/10.1002/jgrd.50472, https://agupubs.onlinelibrary.wiley.com/doi/abs/10.1002/jgrd.50472, 2013.

Praske, E., Crounse, J. D., Bates, K. H., Kurtén, T., Kjaergaard, H. G., and Wennberg, P. O.: Atmospheric Fate of Methyl Vinyl Ketone: Peroxy Radical Reactions with NO and HO_2, J. Phys. Chem. A, 119, 4562–4572, https://doi.org/10.1021/jp5107058, 2015.

Pusede, S. E., Gentner, D. R., Wooldridge, P. J., Browne, E. C., Rollins, A. W., Min, K.-E., Russell, A. R., Thomas, J., Zhang, L., Brune, W. H., Henry, S. B., DiGangi, J. P., Keutsch, F. N., Harrold, S. A., Thornton, J. A., Beaver, M. R., St. Clair, J. M., Wennberg, P. O., Sanders, J., Ren, X., VandenBoer, T. C., Markovic, M. Z., Guha, A., Weber, R., Goldstein, A. H., and Cohen, R. C.: On the temperature dependence of organic reactivity, nitrogen oxides, ozone production, and the impact of emission controls in San Joaquin Valley, California, Atmos. Chem. Phys., 14, 3373–3395, https://doi.org/10.5194/acp-14-3373-2014, 2014.

Pusede, S. E., Duffey, K. C., Shusterman, A. A., Saleh, A., Laughner, J. L., Wooldridge, P. J., Zhang, Q., Parworth, C. L., Kim, H., Capps, S. L., Valin, L. C., Cappa, C. D., Fried, A., Walega, J., Nowak, J. B., Weinheimer, A. J., Hoff, R. M., Berkoff, T. A., Beyersdorf, A. J., Olson, J., Crawford, J. H., and Cohen, R. C.: On the effectiveness of nitrogen oxide reductions as a control over ammonium nitrate aerosol, Atmos. Chem. Phys., 16, 2575–2596, https://doi.org/10.5194/acp-16-2575-2016, https://www.atmos-chem-phys.net/16/2575/2016/, 2016.

Pye, H. O. T., Luecken, D. J., Xu, L., Boyd, C. M., Ng, N. L., Baker, K. R., Ayres, B. R., Bash, J. O., Baumann, K., Carter, W. P. L., Edgerton, E. S., Fry, J. L., Hutzell, W. T., Schwede, D., and Shepson, P. B.: Modeling the Current and Future Roles of Particulate Organic Nitrates in the Southeastern United States, Environ. Sci. Technol., https://doi.org/10.1021/acs.est.5b03738, 2015.

Rindelaub, J. D., McAvey, K. M., and Shepson, P. B.: The photochemical production of organic nitrates from α-pinene and loss via acid-dependent particle phase hydrolysis, Atmos. Environ., 100, 193–201, https://doi.org/10.1016/j.atmosenv.2014.11.010, 2015.

Rollins, A. W., Browne, E. C., Min, K.-E., Pusede, S. E., Wooldridge, P. J., Gentner, D. R., Goldstein, A. H., Liu, S., Day, D. A., Russell, L. M., and Cohen, R. C.: Evidence for NO_x Control Over Nighttime SOA Formation, Science, 337, 1210–1212, https://doi.org/10.1126/science.1221520, http://www.sciencemag.org/content/337/6099/1210, 2012.

Romer, P. S., Duffey, K. C., Wooldridge, P. J., Allen, H. M., Ayres, B. R., Brown, S. S., Brune, W. H., Crounse, J. D., de Gouw, J., Draper, D. C., Feiner, P. A., Fry, J. L., Goldstein, A. H., Koss, A., Misztal, P. K., Nguyen, T. B., Olson, K., Teng, A. P., Wennberg, P. O., Wild, R. J., Zhang, L., and Cohen, R. C.: The lifetime of nitrogen oxides in an isoprene-dominated forest, Atmos. Chem. Phys., 16, 7623–7637, https://doi.org/10.5194/acp-16-7623-2016, http://www.atmos-chem-phys.net/16/7623/2016/, 2016.

Romer, P. S., Duffey, K. C., Wooldridge, P. J., Edgerton, E., Baumann, K., Feiner, P. A., Miller, D. O., Brune, W. H., Koss, A. R., de Gouw, J. A., Misztal, P. K., Goldstein, A. H., and Cohen, R. C.: Effects of temperature-dependent NOx emissions on continental ozone production, Atmos. Chem. Phys., 18, 2601–2614, https://doi.org/10.5194/acp-18-2601-2018, https://www.atmos-chem-phys.net/18/2601/2018/, 2018.

Rosen, R. S., Wood, E. C., Wooldridge, P. J., Thornton, J. A., Day, D. A., Kuster, W., Williams, E. J., Jobson, B. T., and Cohen, R. C.: Observations of total alkyl nitrates during Texas Air Quality Study 2000: Implications for O_3 and alkyl nitrate photochemistry, J. Geophys. Res., 109, D07 303, https://doi.org/10.1029/2003JD004227, http://onlinelibrary.wiley.com/doi/10.1029/2003JD004227/abstract, 2004.

Russell, A. R., Valin, L. C., and Cohen, R. C.: Trends in OMI NO_2 observations over the United States: effects of emission control technology and the economic recession, Atmos. Chem. Phys., 12, 12 197–12 209, https://doi.org/10.5194/acp-12-12197-2012, 2012.

SEAC4RS Science Team: SEAC4RS field campaign data, NASA, https://www-air.larc.nasa.gov/cgi-bin/ArcView/seac4rs, 2014.

SOAS Science Team: SOAS 2013 Centreville site data, NOAA, https://esrl.noaa.gov/csd/groups/csd7/measurements/2013senex/Ground/DataDownload/, 2013.

Sobanski, N., Thieser, J., Schuladen, J., Sauvage, C., Song, W., Williams, J., Lelieveld, J., and Crowley, J. N.: Day and night-time formation of organic nitrates at a forested mountain site in south-west Germany, Atmos. Chem. Phys., 17, 4115–4130, https://www.atmos-chem-phys.net/17/4115/2017/acp-17-4115-2017.html, 2017.

Stelson, A. W. and Seinfeld, J. H.: Relative humidity and temperature dependence of the ammonium nitrate dissociation constant, Atmos. Environ., 16, 983–992, https://doi.org/10.1016/0004-6981(82)90184-6, http://www.sciencedirect.com/science/article/pii/0004698182901846, 1982.

Teng, A. P., Crounse, J. D., Lee, L., St. Clair, J. M., Cohen, R. C., and Wennberg, P. O.: Hydroxy nitrate production in the OH-initiated oxidation of alkenes, Atmos. Chem. Phys., 15, 4297–4316, https://doi.org/10.5194/acp-15-4297-2015, 2015.

Teng, A. P., Crounse, J. D., and Wennberg, P. O.: Isoprene Peroxy Radical Dynamics, J. Am. Chem. Soc., 139, 5367–5377, https://doi.org/10.1021/jacs.6b12838, 2017.

United States Environmental Protection Agency: Air Pollutant Emissions Trends Data, https://www.epa.gov/air-emissions-inventories/air-pollutant-emissions-trends-data, 2018.

Warneke, C., de Gouw, J. A., Holloway, J. S., Peischl, J., Ryerson, T. B., Atlas, E., Blake, D., Trainer, M., and Parrish, D. D.: Multiyear trends in volatile organic compounds in Los Angeles, California: Five decades of decreasing emissions, J. Geophys. Res. Atmos., 117, D00V17, https://doi.org/10.1029/2012JD017899, https://agupubs.onlinelibrary.wiley.com/doi/abs/10.1029/2012JD017899, 2012.

Wennberg, P. O., Bates, K. H., Crounse, J. D., Dodson, L. G., McVay, R. C., Mertens, L. A., Nguyen, T. B., Praske, E., Schwantes, R. H., Smarte, M. D., St Clair, J. M., Teng, A. P., Zhang, X., and Seinfeld, J. H.: Gas-Phase Reactions of Isoprene and Its Major Oxidation Products, Chem. Rev., 118, 3337–3390, https://doi.org/10.1021/acs.chemrev.7b00439, https://doi.org/10.1021/acs.chemrev.7b00439, 2018.

Xiong, F., Borca, C. H., Slipchenko, L. V., and Shepson, P. B.: Photochemical degradation of isoprene-derived 4,1-nitrooxy enal, Atmos. Chem. Phys., 16, 5595–5610, https://doi.org/10.5194/acp-16-5595-2016, 2016.

Xu, L., Guo, H., Boyd, C. M., Klein, M., Bougiatioti, A., Cerully, K. M., Hite, J. R., Isaacman-VanWertz, G., Kreisberg, N. M., Knote, C., Olson, K., Koss, A., Goldstein, A. H., Hering, S. V., Gouw, J. d., Baumann, K., Lee, S.-H., Nenes, A., Weber, R. J., and Ng, N. L.: Effects of anthropogenic emissions on aerosol formation from isoprene and monoterpenes in the southeastern United States, Proc. Natl. Acad. Sci. USA, 112, 37–42, https://doi.org/10.1073/pnas.1417609112, http://www.pnas.org/content/112/1/37, 2015a.

Xu, L., Suresh, S., Guo, H., Weber, R. J., and Ng, N. L.: Aerosol characterization over the southeastern United States using high-resolution aerosol mass spectrometry: spatial and seasonal variation of aerosol composition and sources with a focus on organic nitrates, Atmos. Chem. Phys., 15, 7307–7336, https://doi.org/10.5194/acp-15-7307-2015, https://www.atmos-chem-phys.net/15/7307/2015/, 2015b.

Zare, A., Romer, P. S., Nguyen, T., Keutsch, F. N., Skog, K., and Cohen, R. C.: A comprehensive organic nitrate chemistry: insights into the lifetime of atmospheric organic nitrates, Atmos. Chem. Phys., 18, 15 419–15 436, https://doi.org/10.5194/acp-2018-530, 2018.